The Journal of Immunology

RESEARCH ARTICLE | OCTOBER 15 2019

A Hint of Primitive Mucosal Immunity in Shrimp through *Marsupenaeus japonicus* Gill C-Type Lectin FREE

Rod Russel R. Alenton; ... et. al

J Immunol (2019) 203 (8): 2310–2318.
https://doi.org/10.4049/jimmunol.1900156

A Hint of Primitive Mucosal Immunity in Shrimp through *Marsupenaeus japonicus* Gill C-Type Lectin

Rod Russel R. Alenton,* Keiichiro Koiwai,* Rika Nakamura,* Jumroensri Thawonsuwan,† Hidehiro Kondo,* and Ikuo Hirono*

Lectins are found in most living organisms, providing immune surveillance by binding to carbohydrate ligands. In fishes, C-type lectins were isolated from mucus of respiratory organs (skin and gills), where they aid the mucosal immune response in regulating microbiota and suppressing pathogens. In shrimp, however, no mucosal immunity or any form of gill-specific immune defense has been reported, and most identified C-type lectins are associated with hemocyte cellular and humoral responses. Interestingly, our microarray analysis revealed the localization of highly expressed novel biodefense genes in gills, among which is *Marsupenaeus japonicus* gill C-type lectin (MjGCTL), which we previously reported. Gill mucus collected from *M. japonicus* displayed similar bacterial agglutination ability as observed with recombinant MjGCTL. This agglutinating ability can be attributed to endogenous MjGCTL (nMjGCTL) detected in gill mucus, which was confirmed with an agglutination assay using purified nMjGCTL from gills. In addition, nMjGCTL also promoted in vivo bacterial phagocytosis by hemocytes. In vivo knockdown of MjGCTL resulted in a compromised immune system, which was manifested by impaired agglutination capacity of gill mucus and downregulation of the gill antimicrobial peptides, crustin and penaeidin. Shrimp immunocompromised by MjCGTL knockdown, apparently lost the ability to respond to attaching and penetrating bacteria. This was evident as increased total bacteria and *Vibrio* counts in both gills and hemolymph, which were correlated with low survival during a bacterial challenge. These results reveal immune defense by shrimp gills resembling a primitive form of mucosal immunity. *The Journal of Immunology*, 2019, 203: 2310–2318.

Gills have evolved in various organisms as multifunctional organs involved in respiration, waste excretion, feeding, locomotion, and regulation of osmotic pressure, pH, and hormones (1). The large surface area and semipermeable nature of gills maximizes their efficiency for gas exchange (1, 2). However, constant contact with the aquatic environment has trade-offs, such as vulnerability to ion leakage, uptake of harmful substances, and invasion of pathogens (2, 3). It is through such evolutionary pressures that respiratory organs (i.e., gills, skin, and lungs) in various organisms have evolved convergently to acquire similar traits (1, 3).

One trait shared by invertebrate and vertebrate respiratory organs is mucus production (1, 4, 5). Aside from providing structural integrity and increasing the respiratory surface area, mucus production comprises the first line of defense, known as type I mucosal immunity (6). Mucosal immunity serves immune barrier and surveillance functions on mucosal surfaces, distinguishing beneficial from harmful substances, and accepting or rejecting commensal and pathogenic bacteria (7). Fish mucosal organs (gills, skin, and gut) are lined with epithelium equipped with mucus-producing cells, which are channels for both the innate and adaptive immune defense (8, 9). Knowledge of mucosal immunity in fishes led to cost-effective treatments through oral and immersion administration, known as mucosal vaccination (10). Bacterial uptake activates inflammatory cytokines and adaptive immune responses, suggesting that gills are ideal targets for mucosal vaccination (11).

Mucus secreted by fish gills contains Igs, enzymes, antimicrobial peptides, and pathogen recognition receptors (PRRs) (8, 9, 12). PRRs are key components for surveillance of mucosal surfaces, and a huge group of extracellular PRRs found among metazoans belong to the Ca^{2+}-dependent carbohydrate-binding C-type lectin superfamily (13). C-type lectins have been isolated from fish mucus (skin, gut, and gill) and participate in fish mucosal immunity, recognizing a wide-array of microorganisms (14–18). Two C-type lectins highly expressed in the gills were isolated from gill mucus of the Japanese eel *Anguilla japonica* (19).

Whole-genome studies have revealed an abundance of C-type lectins among invertebrates, where in the absence of adaptive immunity, innate immune systems depend on their pathogen-recognition ability (13). Among crustaceans, a huge number of C-type lectins have been characterized in shrimp, describing

*Graduate School of Marine Science and Technology, Tokyo University of Marine Science and Technology, Minato-ku, Tokyo 108-8477, Japan; and †Songkhla Aquatic Animal Health Research Center, Department of Fisheries, Songkhla 90100, Thailand

ORCIDs: 0000-0002-6015-8649 (R.R.R.A.); 0000-0002-6614-6841 (J.T.); 0000-0002-2355-3121 (I.H.).

Received for publication February 5, 2019. Accepted for publication August 6, 2019.

This study was supported in part by the Japan Science and Technology Agency/Japan International Cooperation Agency, Science and Technology Research Partnership for Sustainable Development, grants-in-aid for scientific research from the Ministry of Education, Culture and Sports, Science and Technology of Japan, and the Heiwa Nakajima Foundation.

Microarray data were submitted to the Gene Expression Omnibus–National Center for Biotechnology Information database under accession number GSE105787.

Address correspondence and reprint requests to Prof. Ikuo Hirono, Graduate School of Marine Science and Technology, Tokyo University of Marine Science and Technology, Minato-ku, Tokyo 108-8477, Japan. E-mail address: hirono@kaiyodai.ac.jp

Abbreviations used in this article: dpi, day post–dsRNA injection; EF, elongation factor; EGFP, enhanced GFP; HI, heart infusion; hpi, hour postimmersion; MAC, minimum agglutination concentration; MjGCTL, *Marsupenaeus japonicus* gill C-type lectin; nMjGCTL, endogenous MjGCTL; PRR, pathogen recognition receptor; rMjGCTL, recombinant MjGCTL; TBSCa, TBS with calcium.

their carbohydrate ligands and binding to microorganisms (20–22). Shrimp C-type lectins are mostly associated with hemocytes, functioning as opsonins to activate both cellular and humoral defense mechanisms, such as release of antimicrobial peptides, prophenol-oxidase activity, respiratory burst, encapsulation, and phagocytosis (23–27). Although some lectins are expressed in shrimp gills (28–30), there have been no reports of gill-specific immune defense and mucosal immunity in shrimp.

We previously reported a novel C-type lectin, *Marsupenaeus japonicus* gill C-type lectin (MjGCTL) gene from kuruma shrimp, *M. japonicus*, which is highly expressed in gills. We investigated the affinity of recombinant MjGCTL (rMjGCTL) for specific carbohydrate ligands, its ability to bind and agglutinate bacteria, and its opsonin activity, promoting hemocyte encapsulation (31). Although these data confirm that MjGCTL functions in the shrimp immune system as a PRR, its endogenous function in gills remains unclear. Speculating on the function of MjGCTL on its organ of localization has also been difficult because of the lack of knowledge on gill-specific immune responses in shrimp.

At present, shrimp gills are understood merely to provide structural support, serving as the extruding site of cellular and humoral response byproducts of hemocytes. However, with the gills constantly exposed to waterborne pathogens, it would be impossible for shrimp to survive without any immune defense in gills. In our present study, microarray analysis identified novel biodefense genes with localized high expression in gills. This evidence of unexplored gill defense mechanisms prompted us to further investigate MjGCTL function with respect to its localization in gills. Based on available knowledge of immune defense in fish gills, C-type lectins provide non-self immune recognition for mucosal immunity (32).

In this study, we provide evidence that gills protect the shrimp through gill mucus equipped with immune molecules such as MjGCTL. Consequently, these results suggest the presence of a gill defense mechanism comparable to mucosal immunity found in higher aquatic organisms, the first evidence, to our knowledge, of gill immune defense and mucosal immunity in shrimp.

Materials and Methods

Experimental organisms

Live *M. japonicus* shrimp were purchased from a farm in Miyazaki Prefecture, Japan. A total of 13 shrimp weighing 25 g were used for protein purification and phagocytosis assay, and 100 shrimp weighing 10 g were used for in vivo challenge experiments. These were kept in tanks with recirculating water maintained at 25˚C and 30 ppt salinity.

Bacterial strains used in this study were Gram-negative, enhanced GFP (EGFP)–expressing *Escherichia coli* and two strains of *Vibrio parahaemolyticus*: acute hepatopancreatic necrosis disease (AHPND) D6 strain and a nonvirulent (N7) strain. Gram-positive, formalin-killed *Streptococcus agalactiae* were also prepared and labeled with PKH67 Green Fluorescent Cell Linker Kit (Sigma-Aldrich) following the manufacturer's protocol.

Microarray analysis

Total RNA from *M. japonicus* hemocytes, gills, hepatopancreas, lymphoid organ, and muscle was extracted using RNAiso reagent (Takara). Extracted total RNA was then purified with an RNeasy Mini Kit (Qiagen), and purity was checked with an Agilent 2200 TapeStation System (Agilent). All samples were prepared in triplicate ($n = 3$), except for hemocytes ($n = 4$).

Total RNA (200 ng) was then reverse transcribed and labeled with Cy3 using a Low Input Quick Amp Labeling kit (Agilent Technologies) and then hybridized on the microarray following the one-color, microarray-based expression analysis protocol. Transcriptomes of the five tissues were then analyzed with an Agilent Gene Expression oligo microarray. Using an 8 × 15K microarray format containing 13,310 probes, complimentary RNA was hybridized for 17 h at 65˚C and then washed for 1 min with buffers 1 and 2 (Agilent Technologies) at 25 and 37˚C, respectively. Upon drying, slides were scanned with a Sure Scan High-Resolution Scanner (Agilent Technologies). Data were extracted from the scanned slides with Agilent Feature Extraction software and imported to GeneSpring GX software (Agilent) for normalization and filtering for expression, flags, and errors. Differentially expressed genes in gills (at least 2-fold higher than normal expression in gills and downregulated in hemocytes, hepatopancreas, lymphoid organ, and muscles) were analyzed, and among those only the immune-related genes were viewed using Heatmap Illustrator (HemI) 1.0 (33). Microarray data were submitted to the Gene Expression Omnibus National Center for Biotechnology Information database with accession number GSE105787 (https://www.ncbi.nlm.nih.gov/geo/query/acc.cgi?acc=GSE105787).

Purification of MjGCTL from gill tissues

Gills were collected from three 25-g *M. japonicus* and homogenized with a glass pestle tissue grinder in 2 ml PBS^+ (PBS with $MgCl_2$, $CaCl_2$). Homogenate was centrifuged at 6000 rpm for 5 min, and 2 ml supernatant was collected. After equilibrating 1 ml bed volume of lactose-agarose beads (Sigma-Aldrich) in PBS^+, 2 ml supernatant was added, mixed in a purification column, and incubated overnight at 4˚C with gentle rotation. The lactose-agarose beads were then washed once with PBS^+ (5× the column volume) and three times with 10 mM EDTA in PBS^+ (5× the column volume). Endogenous MjGCTL (nMjGCTL) was then eluted three times with 500 μl of 50 mM EDTA followed by dialysis with 1 liter of 1× PBS overnight at 4˚C. The purified protein was quantified using DC protein assay (Bio-Rad Laboratories) following the manufacturer's protocol.

Agglutination assay

Bacterial agglutination activity of total soluble protein from the surface of gills and gill tissues (henceforth referred to as gill mucus and gill total protein, respectively) was investigated. To isolate gill mucus, gill tissues were collected, placed in 1.5-ml tubes with PBS^+, vortexed, and collected by filtering. Residual gill tissues were then washed three times and homogenized in PBS^+ and centrifuged at 6000 rpm for 5 min at 4˚C, and supernatant was collected containing total gill protein. The agglutination capacity of both were assayed following published methods (34, 35). Bacterial strains used in the assay were EGFP-expressing *E. coli* and PKH67-labeled *S. agalactiae*. Bacteria were resuspended in TBS with calcium (TBS^{Ca}) (Tris-HCl, pH 7, 100 mM NaCl, and 10 mM $CaCl_2$) at 1×10^8 cells/ml. Ten microliters of bacteria suspension was then incubated with the same volume of MjGCTL (20 μg/ml) at room temperature (25˚C) for 1 h. Agglutination was viewed using fluorescence microscopy (Nikon). rMjGCTL, generated as described in our previous study (31), was used as a positive control and TBS^{Ca} was used as the negative control.

To clearly identify MjGCTL as the main agglutinating factor (agglutinin), the same agglutination assay was performed except that prior to adding bacterial suspension, 10 μl of anti-MjGCTL rabbit serum diluted at 1:500 in TBS^{Ca} was mixed with the same volume of gill mucus and incubated for 30 min at 25˚C. Ten microliters of bacterial suspension was then added and incubated at 25˚C for 1 h. Preimmunized rabbit serum (preserum, control Ab) diluted at the same dilution was used as negative control.

A minimum agglutination concentration (MAC) assay was performed to determine the postknockdown (*In vivo knockdown of MjGCTL by RNA interference*) bacterial agglutination activity of MjGCTL in gill mucus. The agglutination assay was performed as described above using serial dilutions of gill mucus of dsMjGCTL, dsGFP, and PBS-injected shrimp. Gill mucus of naive shrimp was used as a positive control. As a reference for inhibition of agglutination, the MAC assay was also performed on naive shrimp gill mucus after nMjGCTL was inhibited with anti-MjGCTL rabbit serum Ab, as described above. The same procedure was also performed using nonimmunized rabbit serum as the negative control. Results were visualized using fluorescence microscopy (Nikon), where the lowest gill mucus concentration displaying agglutination activity was recorded as the MAC. All agglutination assays were completed in triplicate.

MjGCTL tissue distribution by Western blot analysis

Tissue samples (gills, hemocytes, hepatopancreas, lymphoid organ, muscle, stomach, heart, intestine, nerve, eye, and gill mucous) were harvested from three 25-g shrimp, pooled (~100 mg of each tissue), and homogenized in PBS. Homogenates were mixed with an equal volume

of sample buffer and incubated at 95°C for 5 min. Total protein from each tissue was then subjected to 15% SDS-PAGE and transferred to a nitrocellulose membrane. The membrane was blocked with 4% skimmed milk in 0.05% TBST for 1 h. It was then incubated for 1 h with rabbit serum anti-MjGCTL Ab (Eurofins) diluted to 1:5000 in blocking solution at room temperature with gentle shaking. The membrane was washed four times with 0.05% TBST, incubated for 30 min with anti-rabbit IgG (H chain and L chain), and alkaline phosphatase conjugate (Promega) diluted to 1:5000 in blocking solution at room temperature with gentle shaking. This was followed by three washes with 0.05% TBST. The membrane was then stained with substrate solution containing 5-bromo-4-chloro-3-indolyphosphate and NBT (BCIP/NBT; Sigma-Aldrich) for 2 min and washed with distilled water. Isolated nMjGCTL protein described in *Purification of MjGCTL from gill tissues* was treated similarly.

In vivo knockdown of MjGCTL by RNA interference

A dsRNA template was generated by incorporating the T7 promoter region at both the 5′ and 3′ ends of the MjGCTL primers (Table I). The gene for GFP was used as a nonspecific dsRNA control. dsRNA was generated in vitro through T7 Ribo8MAX Express (Promega) and was purified following manufacturer instructions. Fifty micrograms of dsMjGCTL and dsGFP (dosage: 5 μg/g bodyweight of shrimp) was then injected twice at 24 h intervals, with PBS as the negative control.

To confirm MjGCTL silencing, total RNA and protein from gills were collected separately from three shrimp for each dsRNA treatment group (dsMjGCTL, dsGFP, and PBS) on 1–3 d post–dsRNA injection (dpi). Total RNA was extracted using RNAiso reagent (Takara) and purified with RNeasy Mini Kit (Qiagen). One microgram of total RNA was reverse transcribed using MultiScribe Reverse Transcriptase (Invitrogen) with random primers (Invitrogen). The resulting cDNA template was used for both RT-PCR and quantitative RT-PCR (*Effect of MjGCTL knockdown on expression of other antimicrobial peptides*). RT-PCR thermal cycling conditions were initial denaturation at 95°C for 5 min, followed by 30 cycles of denaturation at 95°C for 30 s, annealing at 55°C for 30 s, and extension at 72°C for 30 s, and then a final extension at 72°C for 5 min. Products were then examined on 1% agarose gel electrophoresis.

In contrast, total protein was subjected to SDS-PAGE and Western blotting using anti-MjGCTL Ab following the procedures described above (*MjGCTL tissue distribution by Western blot analysis*). Anti–β-actin Ab (Novus Biologicals, Littleton, CO) was used as the internal control. Semiquantitative analysis of MjGCTL protein expression was performed with Fiji (ImageJ) software version 2.0 (36), where the expression (based on band intensity) of MjGCTL protein was normalized with the housekeeping protein β-actin. To assess the percentage of knockdown of MjGCTL protein, the normalized expression was calculated as percentage of MjGCTL expression with reference to dsGFP-treated group. Statistical difference was analyzed using Tukey multiple comparisons test with GraphPad Prism 6.0.

Effect of MjGCTL knockdown on bacterial proliferation

The effect of MjGCTL knockdown on the bacterial load in shrimp was assessed in gills and hemolymph of dsMjGCTL, dsGFP, and PBS-treated groups. A total of 90 mg gill tissues and 500 μl of hemolymph suspended in the same volume of anticoagulant (480 mM NaCl, 2.7 mM KCl, 8.1 mM [Na_2HPO_4] 12 H_2O, 1.47 mM KH_2PO_4, pH 7.6, containing 10 mM EDTA) were collected from three shrimp per group at 0 (naive) and 3 dpi (1 d postknockdown). Gill tissues were then suspended in sterile seawater and vortexed. Gill and hemolymph suspensions were serially diluted with sterile seawater and plated on TCBS agar medium to count the *Vibrio* load. Dilutions were also plated on heart infusion (HI) agar with 3% NaCl to count the total bacterial load.

Concurrently, we also assessed the effect of MjGCTL knockdown on *Vibrio* load in gills and hemolymph during immersion with a nonpathogenic (N7) strain of *V. parahaemolyticus*, performed as described in *Challenge test*. Total *Vibrio* colonies were counted at 0, 6, and 12 h postimmersion (hpi) in gills and hemolymph of all treatment groups ($n = 3$), as described above. The data were analyzed with one-way ANOVA with Sidak multiple comparison test using GraphPad Prism 6.0.

In vivo phagocytosis assay by flow cytometry

Opsonization by nMjGCTL was assessed through in vivo phagocytosis assay. Bacterial suspension containing either EGFP-expressing *E. coli* or PKH67-labeled *S. agalactiae* (1×10^8 cells/ml) in TBS^{Ca} was incubated with the purified nMjGCTL (20 μg/ml) for 45 min at 25°C. The resulting suspension (100 μl) of bacteria coated with nMjGCTL was injected to the ventral artery of five shrimp (25 g each) using a 0.5-ml insulin syringe gauge 29. As control, five other shrimp were injected with the bacterial suspension in TBS^{Ca} without nMjGCTL. Hemolymph (500 μl) was then withdrawn 2 h postinjection and mixed with the same volume of anticoagulant 1× PBS with 10 mM EDTA (480 mM NaCl, 2.7 mM KCl, 8.1 mM [Na_2HPO_4] 12 H_2O, 1.47 mM KH_2PO_4, pH 7.6, containing 10 mM EDTA). Fluorescence intensity was then evaluated with a FACSCalibur (Becton-Dickinson), measuring phagocytosis activity at 530/30 nm (FL-1) as the fluorescence of bacteria engulfed by hemocytes. Before measuring phagocytic events, the threshold intensity (FL-1) was set to $>10^1$ using hemolymph (500 μl) withdrawn from naive shrimp as the standard. Hemocyte cells were then selected based on forward and side scatter. Ten thousand events were evaluated with Cell Quest Pro software ver. 5.2.1 (Becton Dickinson). Phagocytic activity was also confirmed through fluorescence microscopy visualizing green fluorescent-labeled bacteria and hemocyte nucleus stained by Hoechst. Results were statistically analyzed using unpaired *t* test with GraphPad Prism 6.0.

Effect of MjGCTL knockdown on expression of other antimicrobial peptides

Postknockdown MjGCTL transcripts as well as transcripts of antimicrobial peptides crustin and penaeidin were quantified by quantitative PCR (qPCR) using THUNDERBIRD SYBR qPCR Mix (TOYOBO). qPCR conditions were 95°C for 1 min, 40 cycles of 95°C for 15 s, and 60°C for 1 min, followed by dissociation analysis step. $Log2^{\Delta\Delta Ct}$ values of target genes, where Ct refers to cycle threshold, were analyzed by normalizing MjGCTL Ct values using elongation factor (EF)–1α as a housekeeping reference gene and with the expression of the target gene on naive shrimp (0 h). Statistical significance was analyzed using one-way ANOVA with Sidak multiple comparison test in GraphPad Prism 6.0.

Challenge test

To investigate whether MjGCTL defense on gills contributes to the prevention of bacterial entry, a survival assay was conducted postknockdown of MjGCTL using a low infection dose based on LD_{20} (i.e., the optimum bacterial concentration that results to a maximum of 20% mortality). For this, a virulent (D6) strain of *V. parahaemolyticus* was cultured in HI medium (3% NaCl) overnight at 30°C. The culture was serially diluted with sterile seawater and inoculated onto HI (3% NaCl) agar plates. After overnight incubation, bacterial colonies were counted. Experimental groups dsMjGCTL and dsGFP were prepared in 20 L seawater (30 ppt), containing 12 shrimp per treatment ($n = 12$). At 3 d posttreatment (1 d postknockdown), all groups were inoculated with 3.0×10^6 CFU/ml final concentration of *V. parahaemolyticus* (D6 strain). Mortality was determined for 7 d and analyzed with Kaplan–Meier survival curve generated with GraphPad Prism 6.0.

Results

Localized high expression of novel biodefense genes in gills

To characterize and identify new gill-specific biodefense genes, we performed microarray analysis of immune-related organs, including gills. All 13,310 spotted genes were expressed. Expression of 101 genes were at least 2-fold higher than normal in gills and at least 2-fold lower than normal in hemocytes, hepatopancreas, lymphoid organ, and muscles. Among the 101 genes, 27 were immune-related, 51 were non–immune-related, and 23 were unknown genes (Tables I, II). As shown in a heat map representation of the 27 immune-related genes, the highest expression occurred in gills (Fig. 1).

MjGCTL protein localization

MjGCTL was among the 27 most highly expressed novel genes in gills (Fig. 1). MjGCTL protein was detected in gills and stomach but not in other organs tested (hemocytes, hepatopancreas, lymphoid organ, muscle, heart, intestine, nerve, and eyes) (Fig. 2). MjGCTL protein's expression was stronger in gills and slightly higher in m.w. as compared with the stomach. Being only

Table I. Primer sequences used for this study

Name	Sequence (5′-3′)
MjGCTL_F	5′-GGCATGGAATAACAGCGAGT-3′
MjGCTL_R	5′-CATTTTGGATGCTGAGCAGA-3′
MjGCTL_qRT_F	5′-GCGCACTAACCTAAACAACACTCTC-3′
MjGCTL_qRT_R	5′-CATAGAAAACGGAGAGGCACTG-3′
MjGCTL_T7_F	5′-TAATACGACTCACTATAGGGCCTAAACAACACTCTCAGCC-3′
MjGCTL_T7_R	5′-TAATACGACTCACTATAGGGCAAAGGGGACTCATGTCAGC-3′
GFP_T7_F	5′-TAATACGACTCACTATAGGGATGGTGAGCAAGGGCGAGGA-3′
GFP_T7_R	5′-TAATACGACTCACTATAGGGTTACTTGTACAGCTCGTCCA-3′
MjGCRUS_qRT_F	5′-GTGGTTTCGGTGGCTTTCCC-3′
MjGCRUS_qRT_R	5′-CGCAGCAGTACGCTTGGTTC-3′
MjPenaeidin_F	5′-TTAGCCTTACTCTGTCAAGTGTACGCC-3′
MjPenaeidin_R	5′-AACCTGAAGTTCCGTAGGAGCCA-3′
EF-1α_F	5′-ATGGTTGTCAACTTTGCCCC-3′
EF-1α_R	5′-TTGACCTCCTTGATCACACC-3′
EF-1α_qRT_F	5′-ATTGCCACACCGCTCACA-3′
EF-1α_qRT_R	5′-TCGATCTTGGTCAGCAGTTCA-3′

expressed in gills and stomach denotes MjGCTL's localization on mucosal surfaces. Together with the unexplored gill immune defense, the higher expression in gills and secretion to the gill mucus prompted us to focus on MjGCTL's gill-specific function.

Gill mucus agglutinates bacteria through nMjGCTL

Following detection of nMjGCTL in gill mucus, we examined whether gill mucus has the ability to agglutinate bacteria, as rMjGCTL did in our previous study (31). Total gill soluble protein, gill mucus, and the positive control rMjGCTL agglutinated EGFP–*E. coli*. To confirm whether nMjGCTL is the main agglutinin on gill mucus, we added anti-MjGCTL serum Ab for competitive binding. This inhibited agglutination activity of the three above-mentioned protein treatments, in contrast to the negative control using preserum Ab or buffer (TBS^{Ca}) alone (Fig. 3). These results confirm that nMjGCTL in gill mucus is responsible for the bacterial agglutination capacity of gill mucus.

To isolate nMjGCTL activity from bioactivities of other proteins that may be present in gills, native MjGCTL was purified from gill tissues. nMjGCTL was successfully isolated from gill tissues using lactose-agarose protein chromatography, confirmed by both SDS-PAGE and Western blot using anti-MjGCTL serum Ab (Fig. 4A, 4B). MjGCTL eluted from gill tissues had a molecular mass of ~45 kDa, as shown by SDS-PAGE (Fig. 4A) and Western blot (Fig. 4B). The activity of eluted MjGCTL was confirmed through the agglutinated Gram-positive PKH67-labeled *S. agalactiae* and Gram-negative EGFP–*E. coli* (Fig. 4C).

MjGCTL knockdown impairs bacterial agglutinating activity in gills

MjGCTL knockdown was confirmed both at both mRNA and protein levels. Fewer transcripts of MjGCTL were detected by semiquantitative RT-PCR at 1 dpi, whereas complete knockdown was observed at 2 and 3 dpi (Fig. 5A). MjGCTL protein expression after knockdown with cognate dsRNA was lower compared with dsGFP and PBS-injected shrimp at 1 dpi (Fig. 5B). Postknockdown protein expression of MjGCTL in Fig. 5B was quantified using image-based analysis of the band intensity of MjGCTL normalized with housekeeping protein β-actin. MjGCTL protein expression on dsMjGCTL group was significantly ($p < 0.01$) lower than dsGFP, having only 32, 19, and 10% expression of dsGFP at 1–3 dpi, respectively (Fig. 5C).

Gill mucus from MjGCTL knockdown shrimp had less agglutinating capacity compared with dsGFP or PBS-injected shrimp (Fig. 6A). Complete loss of agglutination activity was not observed (Fig. 6A), which is expected, as MjGCTL protein was not completely silenced (Fig. 5B). For this, MAC of gill mucus from all treatment groups was compared. The MAC

Table II. Microarray analysis of novel shrimp biodefense genes

Genes	Count
Total spotted	13,310
Expressed	13,310
Differentially expressed in gills	101
Immune-related	27
Others	51
Unknown	23

Summary of results of a microarray analysis of novel biodefense genes in *M. japonicus* hemocytes, gills, hepatopancreas, lymphoid organs, and muscles.

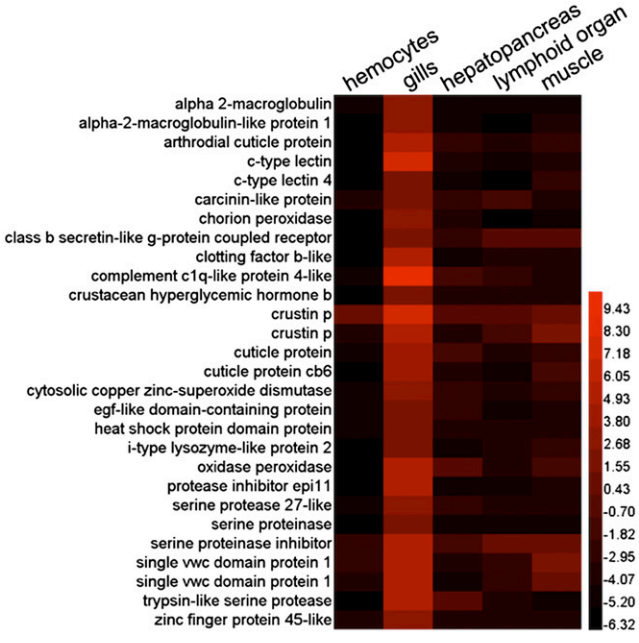

FIGURE 1. Highly expressed novel immune-related genes in gills. Microarray analysis heat map comparing the expressions of 27 differentially expressed biodefense genes in various immune-related tissues. Expression of 27 biodefense genes in gills exceeded that in other immune-related tissues by at least 2-fold. Analysis was performed on RNA from *M. japonicus* hemocytes, gills, hepatopancreas, lymphoid organ, and muscle. All tissue samples were prepared in triplicates ($n = 3$), except for hemocytes ($n = 4$).

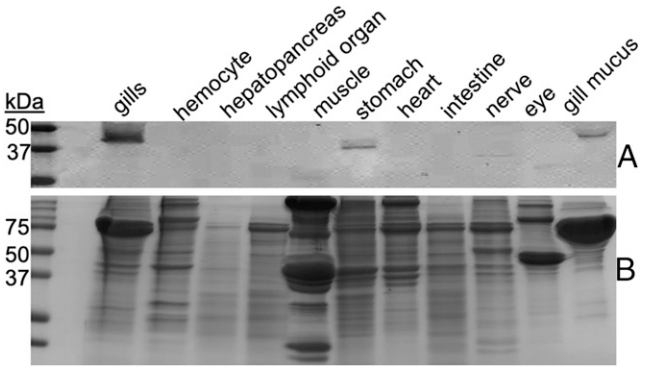

FIGURE 2. MjGCTL is localized in mucosal organs. (**A**) Western blot detection of MjGCTL on various pooled ($n = 3$) tissues using anti-MjGCTL rabbit serum Ab. (**B**) Total protein concentration of each tissue was normalized by SDS-PAGE as loading control.

of gill mucus was significantly higher among MjGCTL knockdown shrimp compared with controls, indicating that MjGCTL knockdown results in impaired agglutinating activity (Fig. 6B).

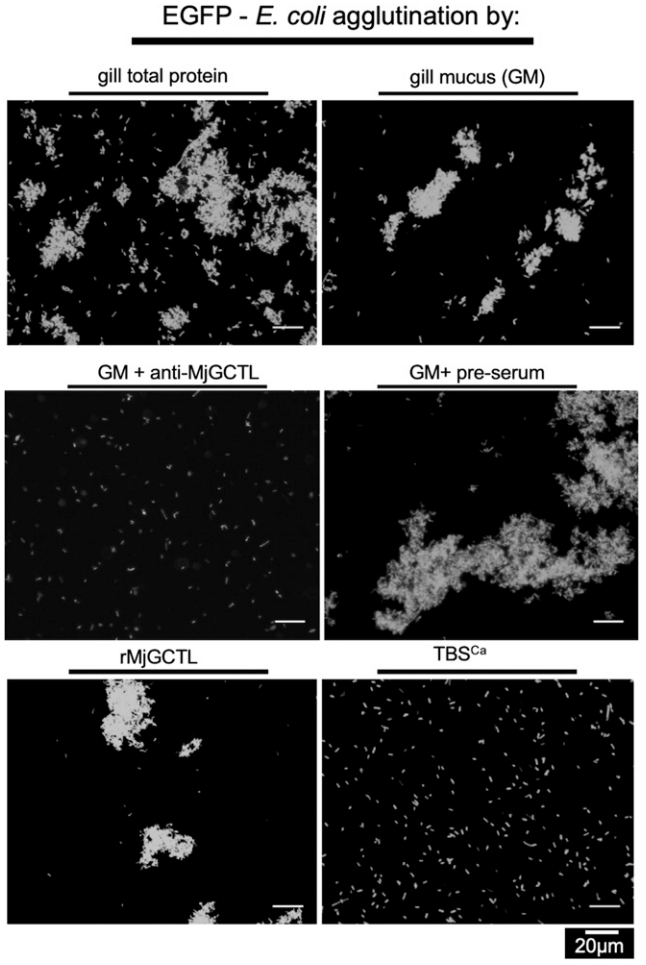

FIGURE 3. nMjGCTL secreted by gills agglutinates bacteria. EGFP-expressing *E. coli* agglutinated by total protein from gills, as well as by gill mucus. Agglutination inhibition by rabbit serum anti-MjGCTL Ab neutralizing agglutination activity, with nonimmunized rabbit serum as a negative control. rMjGCTL was used as a positive control and TBS^{Ca} was used as a negative control. Each image represents an agglutination assay performed in triplicate.

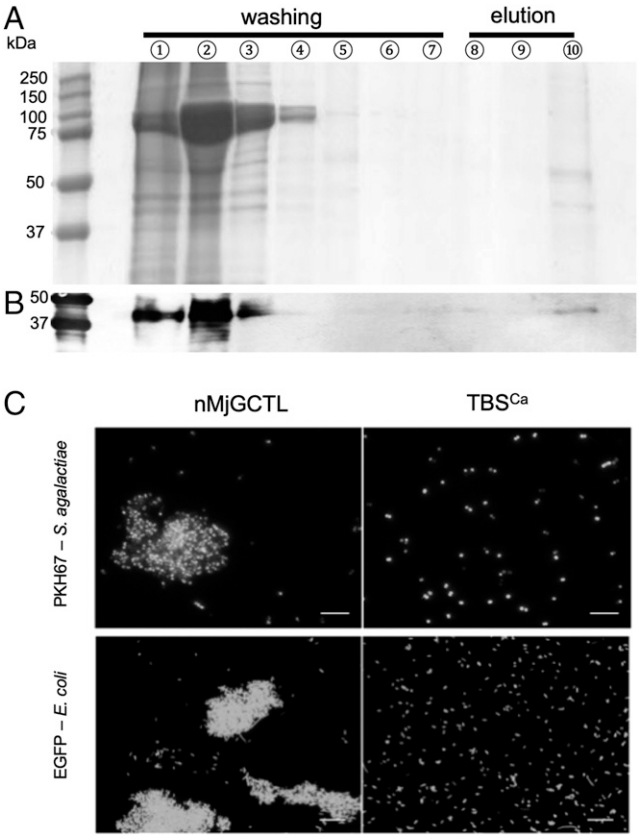

FIGURE 4. Purified nMjGCTL agglutinates bacteria. (**A**) SDS-PAGE showing elution of native MjGCTL from lactose-agarose beads. Lane 1, flow-through; lanes 2–4, fractions eluted with PBS (2–4); lanes 5–7, fractions eluted with 10 mM EDTA; lanes 8–10, fractions eluted with 50 mM EDTA. (**B**) Eluted MjGCTL was confirmed using Western blot analysis using anti-MjGCTL rabbit serum. (**C**) Bacterial agglutination activity of eluted MjGCTL against PHK67-labeled *S. agalactiae* and EGFP-expressing *E. coli*, with only TBS^{Ca} as a negative control. Each image is a representative of agglutination experiments done in triplicates.

MjGCTL is involved in regulating gill and hemolymph bacterial load

Total bacterial load and *Vibrio* count in gills increased upon MjGCTL knockdown, although not significantly (Fig. 7A, left graph). For dsMjGCTL, *Vibrio* count was 4.0×10^5 CFU/ml, and the control naive, dsGFP, and PBS groups were 1.6×10^4, 7×10^4, and 3.0×10^5 CFU/ml, respectively. Similarly, total bacteria count for dsMjGCTL group was 1.0×10^6 CFU/ml, which is also higher than the control groups naive, dsGFP, and PBS, at 5.2×10^5, 1.6×10^5, and 6.6×10^5, respectively. In the hemolymph, however, *Vibrio* growth was detected only among MjGCTL knockdown shrimp (dsMjGCTL), where the total bacteria count was also significantly ($p < 0.01$) higher than the dsGFP group (Fig. 7A, right graph). *Vibrio* and total bacteria count in gills of dsMjGCTL group were 2.3×10^3 and 1.0×10^4, respectively. In contrast, no CFU *Vibrio* and total bacteria were observed among all control groups except dsGFP total bacteria count, with 6.0×10^2 CFU/ml.

Changes in *Vibrio* load in the presence or absence of MjGCTL were also measured in gills and hemolymph after 6 and 12 h immersion with *V. parahaemolyticus* (Fig. 7B, left graph), which may represent *Vibrio* attachment to gills and uptake in hemolymph (Fig. 7B, right graph). This is evident when comparing *Vibrio* load in both gills and hemolymph of nonimmersed (Fig. 7A) and immersed (Fig. 7B), where the counts are higher in the latter with *V. parahemolyticus* introduced in water. Significant ($p < 0.01$)

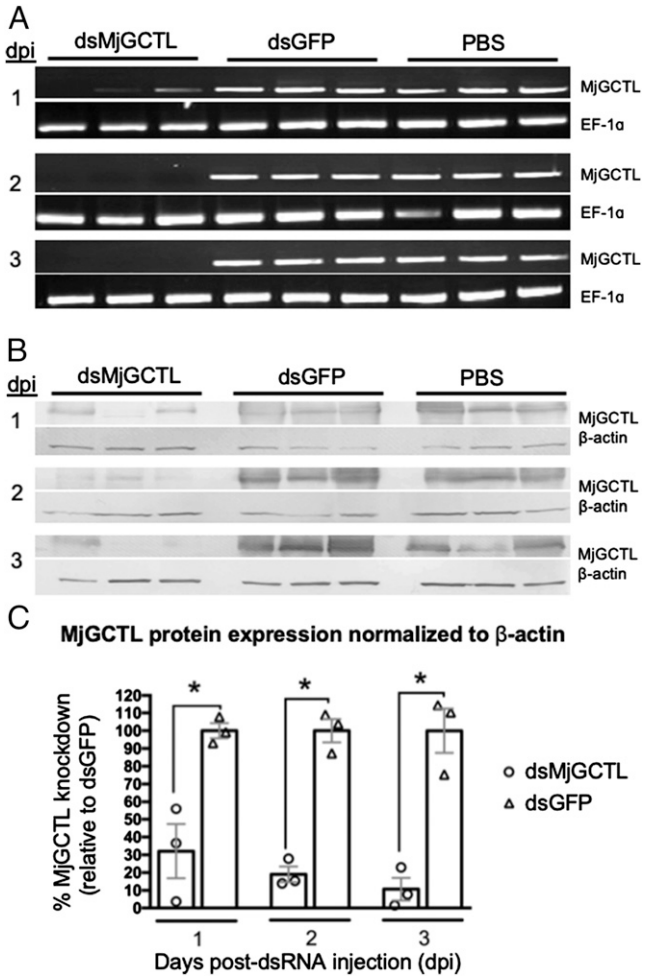

FIGURE 5. RNA interference knockdown of MjGCTL in vivo in both mRNA and protein level. (**A**) RT-PCR analysis of MjGCTL transcripts in gills at 1, 2, and 3 d dpi of dsMjGCTL, dsGFP (dsRNA control), and PBS (negative control) using 5 μg/g of shrimp dsRNA dosage. (**B**) Knockdown of MjGCTL protein by cognate dsRNA at days 2 and 3 post–dsRNA injection, using β-actin as a loading control. Both RNA and protein samples were collected from three separate samples ($n = 3$) for each treatment group. (**C**) Image-based semiquantitative analysis of postknockdown expression of MjGCTL protein normalized with housekeeping protein β-actin. MjGCTL knockdown is expressed as percentage based on the average MjGCTL expression in dsGFP control group. Significant difference ($p < 0.01$) between dsMjGCTL and dsGFP groups are denoted by an asterisk (*).

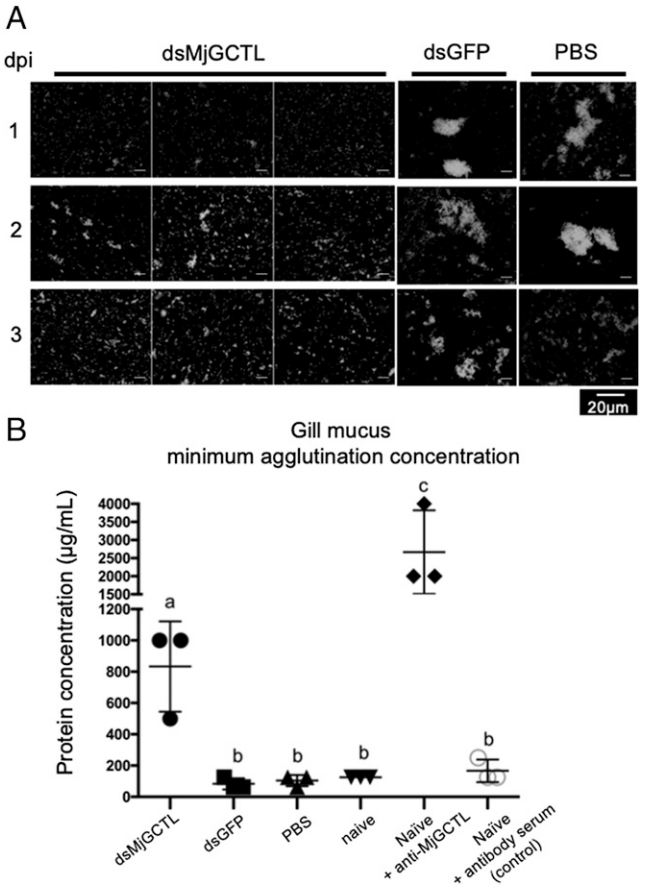

FIGURE 6. MjGCTL knockdown impairs the bacteria-agglutinating capacity of gill mucus. (**A**) EGFP-expressing *E. coli* agglutination by gill mucus obtained at 1–3 dpi of dsMjGCTL, dsGFP, and PBS ($n = 3$). (**B**) Quantification of agglutination inhibition through MAC of gill mucus from all treatment groups (obtained 3 dpi). As control experiments, gill mucus from naive shrimp was neutralized using anti-MjGCTL Ab serum and preserum as negative Ab control. Letters a–c denote statistical differences ($p < 0.01$) between the groups.

increase in *Vibrio* load in gills during 6–12 h after *Vibrio* immersion was only observed among dsMjGCTL, increasing from 4.0×10^6 to 6×10^7 CFU/ml. In contrast, dsGFP and PBS groups only increased from 9.0×10^6 to 3.2×10^7 and 6.0×10^5 to 5×10^6 CFU/ml, respectively (Fig. 7B, left graph). *Vibrio* load in the hemolymph of all treatment groups increased substantially from 6 to 12 h after *Vibrio* immersion (Fig. 7B, right graph), with a 100-fold increase for dsMjGCTL, 30-fold for dsGFP, and 15-fold for PBS groups. Comparing the *Vibrio* load between treatments at 12 hpi, dsMjGCTL group with 4.0×10^5 CFU/ml was significantly ($p < 0.05$) higher compared with the control dsGFP and PBS groups, with 1.6×10^5 and 6.0×10^4, respectively. *Vibrio* counts on the naive shrimp were the lowest, with 2.3×10^3 CFU/ml on the gills, and no colonies were observed from the hemolymph.

Opsonic effect of MjGCTL

Addition of nMjGCTL increased the phagocytic rate in vivo for PKH67-labeled *S. agalactiae* but not for *E. coli* (Fig. 8A). A peak after the 10^1 FL1-H threshold of hemocyte population was detected as phagocytosed PHK67-labeled *S. agalactiae* in the presence of nMjGCTL but not in the control lacking nMjGCTL (Fig. 8B). Phagocytic activity was also confirmed immunohistochemically (Fig. 8C).

MjGCTL is involved in regulation of antimicrobial peptides

Quantitative RT-PCR showed that MjGCTL transcripts in MjGCTL knockdown shrimp at 3 dpi were significantly less abundant than in the dsGFP-treated control group (Fig. 9A). Two antimicrobial peptides that are expressed in gills of *M. japonicus* (crustin and penaeidin) were also significantly downregulated upon MjGCTL knockdown (Fig. 9B).

Effect of MjGCTL knockdown on shrimp survival

At 7 d postimmersion with a low concentration of the virulent strain of *V. parahaemolyticus*, survival of MjGCTL knockdown shrimp was reduced to 20 and 0% for the first and second challenge test, respectively (Fig. 10). In contrast, a control group treated with dsGFP maintains 90% survival for both challenge tests. The two separate challenge tests showed significant difference ($p < 0.01$ and $p < 0.001$, respectively) between dsMjGCTL and dsGFP-treated groups using Kaplan–Meier survival curve analysis, indicating a reduced survival among shrimp in the absence of MjGCTL during infection (Fig. 10).

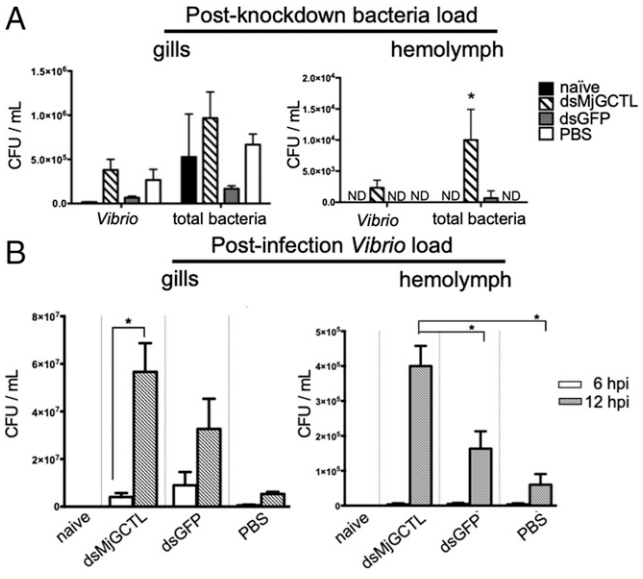

FIGURE 7. MjGCTL-knockdown results in bacterial proliferation. (**A**) The effect of MjGCTL-knockdown on (noninfected) shrimp total *Vibrio* and bacteria load shown through CFU count on gill tissues and hemolymph of naive, 3 d post–dsMjGCTL, dsGFP, and PBS treatment groups. (**B**) Effect of MjGCTL knockdown on bacterial growth through *Vibrio* CFU count on gills and hemolymph at 0, 6, and 12 hpi with *V. parahaemolyticus* (N7-strain). The challenge test was conducted at 3 dpi MjGCTL-knockdown, dsGFP and PBS treatment. Significant difference ($p < 0.01$) are denoted by an asterisk (*).

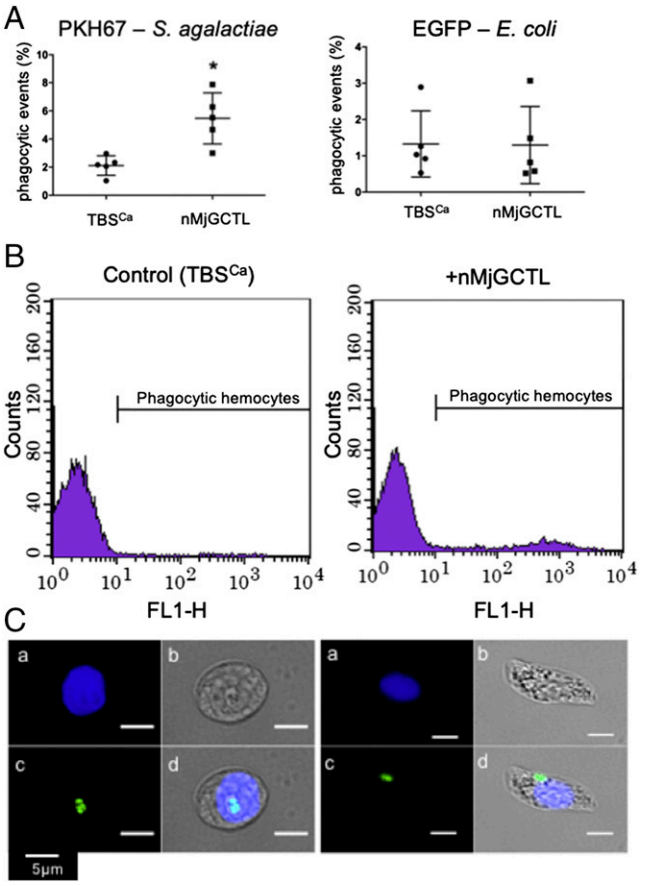

FIGURE 8. Purified native MjGCTL promotes phagocytosis in vivo. (**A**) In vivo phagocytosis assay by flow cytometry using *S. agalactiae* labeled with PKH67 and EGFP–*E. coli*. Significant differences ($p < 0.01$) are indicated by an asterisk (*). (**B**) A representative histogram of FCM results ($n = 5$) on the phagocytic activity of MjGCTL against PKH67–*S. agalactiae*. Threshold intensity (FL-1) was set to $<10^1$ representing the nonfluorescent (i.e., nonphagocytic) hemocytes control population using hemolymph withdrawn from naive shrimp. Hemocyte cells were then selected based on forward and side scatter. Ten thousand events were evaluated. (**C**) Fluorescence microscopy images of representative phagocytic activity against PKH67–*S. agalactiae* showing a hemocyte nucleus stained with Hoechst (a), PKH67-stained *S. agalactiae* (b), a bright-field image of a hemocyte (c), and the merged image of a–c demonstrating the phagocytic activity (d).

Discussion

Functional evidence for mucosal immunity among invertebrates is still lacking, despite the emergence of mucosal surfaces that are traceable back to early metazoans (37). Mucosal immunity is unique to mucosal surfaces, which are found on organs constantly exposed to the external environment, such as digestive, respiratory, and reproductive organs. Studies focusing on gut-specific immune mechanisms reveal some similarities between vertebrate mucosal immunity and some invertebrate immune mechanisms (38, 39). In this study, we investigated invertebrate gills and discovered gill-specific immune mechanisms, suggesting the presence of a primitive form of mucosal immunity.

Gills are considered mucosal surfaces and immune-related organs in shrimp (4, 40, 41). However, gill-specific immune mechanisms have not yet been described among invertebrates. In our microarray data, however, we observed localization of highly expressed, novel, biodefense genes on the gills of *M. japonicus* shrimp (Fig. 1). Most of these genes encode the same type of immune effector molecules that contribute to vertebrate gut mucosal immunity (38). Among them are C-type lectins, lysozymes, reactive oxygen species, and antimicrobial peptides. This prompted us to hypothesize that invertebrates have gill-specific immune defense, potentially resembling the mechanism of vertebrate mucosal immunity.

Previously, we described MjGCTL as a potential PRR using rMjGCTL in vitro (31). In the current study, we found MjGCTL to be one of the gill-specific novel biodefense genes (Fig. 1), which might signify its involvement in an undescribed gill defense mechanism. Supporting our hypothesis, nMjGCTL protein is localized in mucosal organs gills and stomach (Fig. 2). nMjGCTL's higher expression in gills and its presence in secreted gill mucus further reveal the role of MjGCTL in a gill immune mechanism. These characteristics of MjGCTL fit the description of vertebrate type I mucosal immunity (6). Also belonging to mucosal type I mucosal immunity are C-type lectins isolated from fish respiratory organs (14–19). Interestingly, two of these were isolated from gill mucus of the Japanese eel, *A. japonica*, and share the same tissue expression profile as MjGCTL (19). These results not only suggest MjGCTL's function being localized on mucosal surfaces, but also provide evidence of existing mucosal immunity in shrimp gills.

To further investigate the link between gill defense and mucosal immunity, we needed to reveal MjGCTL's endogenous function in gills. First, we found that both gill mucus and total gill protein lysate have the same bacterial agglutination ability as rMjGCTL (Fig. 3). To confirm nMjGCTL as the main agglutinin in gill mucus, we neutralized nMjGCTL by competitive binding with anti-MjGCTL Ab, resulting in the inhibition of bacterial agglutination (Fig. 3). We then replicated the agglutination assay results using isolated nMjGCTL from gills, where the activity of purified nMjGCTL demonstrated bacterial agglutination capacity (Fig. 4). These results are corroborated by the in vivo knockdown of MjGCTL (Fig. 5), resulting in impaired agglutinating activity of gill mucus

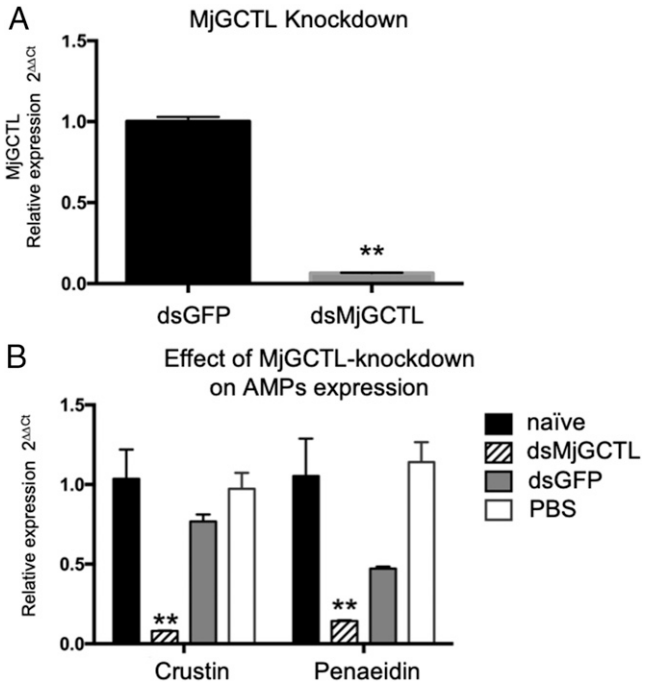

FIGURE 9. MjGCTL is involved in regulation of antimicrobial peptides (AMP). (**A**) MjGCTL mRNA level at 3 d postinjection of control dsGFP and sequence-specific dsMjGCTL and its effect on (**B**) mRNA levels of the AMPs crustin and penaeidin 3 d after dsMjGCTL, dsGFP, and PBS, with untreated shrimp as an additional control. All samples were prepared in triplicates ($n = 3$). A double asterisk (**) denotes a significant difference ($p < 0.001$) using t tests and ANOVA.

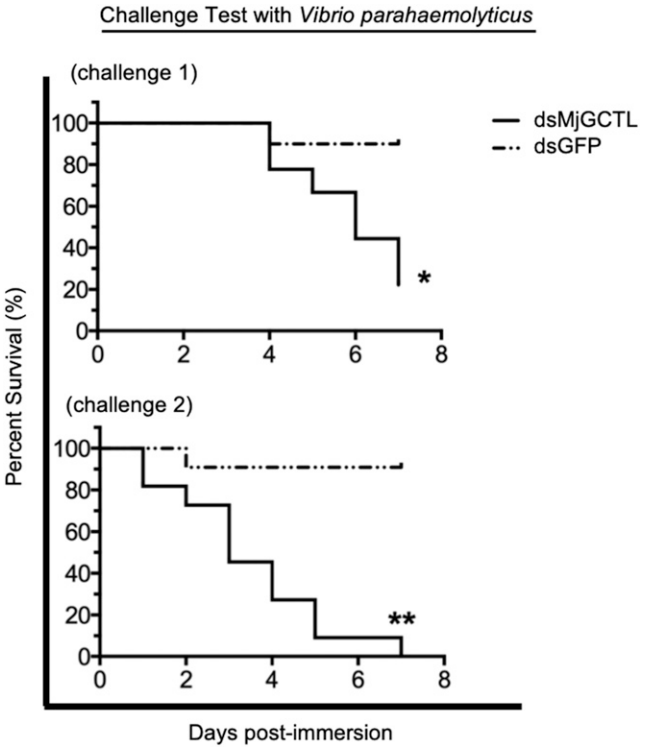

FIGURE 10. MjGCTL knockdown decreases shrimp survival during infection. Bacterial challenge with a virulent strain (D6) of *V. parahaemolyticus* after dsMjGCTL and dsGFP treatment, recorded up to 7 d postimmersion. Both survival curves were obtained from separate challenge tests. A single asterisk (*) denotes a significant difference at $p < 0.01$ and double asterisk (**) at $p < 0.001$ based on Kaplan–Meier survival analysis.

(Fig. 6). Demonstrated here is the gill defense using secreted mucus equipped with the mucosal lectin, MjGCTL.

The use of lectins to eliminate or regulate bacteria is an ancient mechanism, known from both vertebrate and nonvertebrate models (42–45). For instance, bacteria maintenance and endosymbiosis are achieved with the binding of the lectin discoidin I, which protects and extends the retention of bacteria in the social amoeba *Dictyostelium discoideum* (44). In the mosquito *Aedes aegypti*, some members of the gut microbiome use C-type lectins to overcome host immune responses by counteracting antimicrobial peptide activity (45). MjGCTL is also involved in bacterial regulation, as total bacterial and *Vibrio* load increased in both gills and hemolymph of MjGCTL knockdown shrimp (Fig. 7A), indicating MjGCTL's role in maintaining homeostasis. In the absence of MjGCTL, exposure to *V. parahaemolyticus* resulted in a significant increase in the *Vibrio* load in gills and hemolymph from 6 to 12 hpi (Fig. 7B). In this study we demonstrate that, as with the aforementioned invertebrate lectins, MjGCTL appears to also function in lectin-mediated mucosal immunity.

Our data show that without MjGCTL, bacteria that the immune system would normally suppress can proliferate, and that during infection, more bacteria colonize or adhere to gill surfaces. In contrast, control groups maintained lower bacterial counts. The *Vibrio* count in hemolymph allowed us to assess the number of bacteria that could possibly have penetrated the shrimp during immersion. Six hours after immersion, all groups of shrimp had very few *Vibrio* CFUs, which suggests that 6 h was not enough for bacteria to penetrate the host. The lower *Vibrio* count in hemolymph was expected because the hemolymph has the capacity to clear bacteria (46, 47). Nonetheless, at 12 hpi, the *Vibrio* count in hemolymph of MjGCTL knockdown shrimp increased significantly (Fig. 7B). These results show that MjGCTL knockdown in the gills allows more bacteria to penetrate the gills.

Unrestricted bacterial burden caused by MjGCTL knockdown also manifests a mechanism by which MjGCTL eliminates bacteria or prevents their growth. The lectin-complement pathway has been described in many invertebrates, in which binding of bacteria by lectins activates host humoral and cellular defenses (48). This is observed in another shrimp lectin Fclec4, which promotes clearance of pathogenic bacteria in vivo (30). nMjGCTL, in contrast, promoted in vivo phagocytosis of PKH67-labeled *S. agalactiae* (Fig. 8). Although unlike the hepatopancreas, the gills have no known specialized phagocytic cells (49), it was recently discovered that *M. japonicus* gills have sessile (i.e., noncirculating) hemocytes (50) that may act as phagocytic cells for MjGCTL. The possible activation of the lectin-complement pathway by MjGCTL is seen through its involvement in antimicrobial peptide expression regulation, as crustin and penaeidin were downregulated in response to MjGCTL knockdown (Fig. 9). This is further corroborated by the survival assay, where silencing MjGCTL leads to reduced survival during infection (Fig. 10). These results demonstrated that without MjGCTL, gills are overburdened with penetrating bacteria that soon breach the shrimp's defenses, causing mortality.

Taken together, our study provides functional evidence that MjGCTL confers a lectin-mediated defense through the gill mucus. MjGCTL contributes to the shrimp's external defenses from the gill surface, where MjGCTL agglutinates and tags invading pathogen for the destruction by other immune effectors present in gills. In the event that bacteria are able to penetrate the shrimp, opsonization with MjGCTL promotes phagocytosis by hemocytes. In addition, MjGCTL's involvement in regulating the expression

of antimicrobial peptides may contribute to the prevention of bacterial proliferation. These immune functions of MjGCTL contribute to shrimp survival during infection.

To our knowledge, this study provides the first evidence of gill-specific immune defense among invertebrates. MjGCTL's immune function in gill mucus reveals a link between previously undescribed gill and mucosal immune mechanisms in shrimp. Our study suggests that shrimp gills possess a defense mechanism resembling a primitive form of mucosal immunity.

Disclosures

The authors have no financial conflicts of interest.

References

1. Maina, J. N. 2002. Structure, function and evolution of the gas exchangers: comparative perspectives. *J. Anat.* 201: 281–304.
2. Koppang, E. O., A. Kvellestad, and U. Fischer. 2015. Fish mucosal immunity: gill. In *Mucosal Health in Aquaculture*. Elsevier, Amsterdam, p. 93–133
3. Xu, Z., F. Takizawa, D. Parra, D. Gómez, L. von Gersdorff Jørgensen, S. E. LaPatra, and J. O. Sunyer. 2016. Mucosal immunoglobulins at respiratory surfaces mark an ancient association that predates the emergence of tetrapods. *Nat. Commun.* 7: 10728.
4. Foster, C. A., and H. D. Howse. 1978. A morphological study on gills of the brown shrimp, Penaeus aztecus. *Tissue Cell* 10: 77–92.
5. Cieluch, U., K. Anger, M. Charmantier-daures, and G. Charmantier. 2007. Osmoregulation and immunolocalization of Na^+/K^+-ATPase during the ontogeny of the mitten crab *Eriocheir sinensis* (Decapoda, Grapsoidea). *Mar. Ecol. Prog. Ser.* 329: 169–178.
6. Iwasaki, A. 2007. Mucosal dendritic cells. *Annu. Rev. Immunol.* 25: 381–418.
7. Sato, S., and H. Kiyono. 2012. The mucosal immune system of the respiratory tract. *Curr. Opin. Virol.* 2: 225–232.
8. Gomez, D., J. O. Sunyer, and I. Salinas. 2013. The mucosal immune system of fish: the evolution of tolerating commensals while fighting pathogens. *Fish Shellfish Immunol.* 35: 1729–1739.
9. Wilson, J. M., and P. Laurent. 2002. Fish gill morphology: inside out. *J. Exp. Zool.* 293: 192–213.
10. Vervarcke, S., F. Ollevier, R. Kinget, and A. Michoel. 2005. Mucosal response in African catfish after administration of *Vibrio anguillarum* O2 antigens via different routes. *Fish Shellfish Immunol.* 18: 125–133.
11. Kato, G., T. Takano, T. Sakai, T. Matsuyama, and C. Nakayasu. 2013. *Vibrio anguillarum* bacterin uptake via the gills of Japanese flounder and subsequent immune responses. *Fish Shellfish Immunol.* 35: 1591–1597.
12. Alexander, J. B., and A. Ingram. 1992. Noncellular nonspecific defence mechanisms of fish. *Annu. Rev. Fish Dis.* 2: 249–279.
13. Zelensky, A. N., and J. E. Gready. 2005. The C-type lectin-like domain superfamily. *FEBS J.* 272: 6179–6217.
14. Tsutsui, S., Y. Komatsu, T. Sugiura, K. Araki, and O. Nakamura. 2011. A unique epidermal mucus lectin identified from catfish (Silurus asotus): first evidence of intelectin in fish skin slime. *J. Biochem.* 150: 501–514.
15. Tsutsui, S., K. Iwamoto, O. Nakamura, and T. Watanabe. 2007. Yeast-binding C-type lectin with opsonic activity from conger eel (*Conger myriaster*) skin mucus. *Mol. Immunol.* 44: 691–702.
16. Tsutsui, S., Y. Dotsuta, A. Ono, M. Suzuki, H. Tateno, J. Hirabayashi, and O. Nakamura. 2015. A C-type lectin isolated from the skin of Japanese bullhead shark (*Heterodontus japonicus*) binds a remarkably broad range of sugars and induces blood coagulation. *J. Biochem.* 157: 345–356.
17. Tasumi, S., W. J. Yang, T. Usami, S. Tsutsui, T. Ohira, I. Kawazoe, M. N. Wilder, K. Aida, and Y. Suzuki. 2004. Characteristics and primary structure of a galectin in the skin mucus of the Japanese eel, Anguilla japonica. *Dev. Comp. Immunol.* 28: 325–335.
18. Suzuki, Y., S. Tasumi, S. Tsutsui, M. Okamoto, and H. Suetake. 2003. Molecular diversity of skin mucus lectins in fish. *Comp. Biochem. Physiol. B Biochem. Mol. Biol.* 136: 723–730.
19. Mistry, A. C., S. Honda, and S. Hirose. 2001. Structure, properties and enhanced expression of galactose-binding C-type lectins in mucous cells of gills from freshwater Japanese eels (*Anguilla japonica*). *Biochem. J.* 360: 107–115.
20. Marques, M. R. F., and M.A. Barracco 2000. Lectins, as non-self-recognition factors, in crustaceans. *Aquaculture* 191: 23–44.
21. Vazquez, L., J. Alpuche, G. Maldonado, C. Agundis, A. Pereyra-Morales, and E. Zenteno. 2009. Review: immunity mechanisms in crustaceans. *Innate Immun.* 15: 179–188.
22. Wang, X. W., and J. X. Wang. 2013. Diversity and multiple functions of lectins in shrimp immunity. *Dev. Comp. Immunol.* 39: 27–38.
23. Söderhäll, K., and L. Cerenius. 1992. Crustacean immunity. *Annu. Rev. Fish Dis.* 2: 3–23.
24. Yu, X. Q., and M. R. Kanost. 2004. Immulectin-2, a pattern recognition receptor that stimulates hemocyte encapsulation and melanization in the tobacco hornworm, *Manduca sexta. Dev. Comp. Immunol.* 28: 891–900.
25. Yu, X. Q., and M. R. Kanost. 2000. Immulectin-2, a lipopolysaccharide-specific lectin from an insect, *Manduca sexta*, is induced in response to gram-negative bacteria. *J. Biol. Chem.* 275: 37373–37381.
26. Yu, X. Q., E. Ling, M. E. Tracy, and Y. Zhu. 2006. Immulectin-4 from the tobacco hornworm *Manduca sexta* binds to lipopolysaccharide and lipoteichoic acid. *Insect Mol. Biol.* 15: 119–128.
27. Cerenius, L., P. Jiravanichpaisal, H.-p. Liu, and I. Soderhall. 2010. Crustacean immunity. In *Invertebrate Immunity. Advances in Experimental Medicine and Biology.* K. Söderhäll, ed. Vol. 708. Springer, Boston, MA, p. 239–259.
28. Costa, F. H., N. S. Valença, A. R. Silva, G. A. Bezerra, B. S. Cavada, and G. Rádis-Baptista. 2011. Cloning and molecular modeling of *Litopenaeus vannamei* (Penaeidae) C-type lectin homologs with mutated mannose binding domain-2. *Genet. Mol. Res.* 10: 650–664.
29. Junkunlo, K., A. Prachumwat, A. Tangprasittipap, S. Senapin, S. Borwornpinyo, T. W. Flegel, and K. Sritunyalucksana. 2012. A novel lectin domain-containing protein (LvCTLD) associated with response of the whiteleg shrimp *Penaeus* (*Litopenaeus*) *vannamei* to yellow head virus (YHV). *Dev. Comp. Immunol.* 37: 334–341.
30. Wang, X. W., X. W. Zhang, W. T. Xu, X. F. Zhao, and J. X. Wang. 2009. A novel C-type lectin (FcLec4) facilitates the clearance of *Vibrio anguillarum* in vivo in Chinese white shrimp. *Dev. Comp. Immunol.* 33: 1039–1047.
31. Alenton, R. R., K. Koiwai, K. Miyaguchi, H. Kondo, and I. Hirono. 2017. Pathogen recognition of a novel C-type lectin from *Marsupenaeus japonicus* reveals the divergent sugar-binding specificity of QAP motif. *Sci. Rep.* 7: 45818.
32. Brinchmann, M. F., D. M. Patel, N. Pinto, and M. H. Iversen. 2018. Functional aspects of fish mucosal lectins - interaction with non-self. *Molecules* DOI: 10.3390/molecules23051119.
33. Deng, W., Y. Wang, Z. Liu, H. Cheng, and Y. Xue. 2014. HemI: a toolkit for illustrating heatmaps. *PLoS One* 9: e111988.
34. Luo, T., H. Yang, F. Li, X. Zhang, and X. Xu. 2006. Purification, characterization and cDNA cloning of a novel lipopolysaccharide-binding lectin from the shrimp Penaeus monodon. *Dev. Comp. Immunol.* 30: 607–617.
35. Zhang, X. W., Y. Wang, X. W. Wang, L. Wang, Y. Mu, and J. X. Wang. 2016. A C-type lectin with an immunoglobulin-like domain promotes phagocytosis of hemocytes in crayfish *Procambarus clarkii. Sci. Rep.* 6: 29924.
36. Schindelin, J., I. Arganda-Carreras, E. Frise, V. Kaynig, M. Longair, T. Pietzsch, S. Preibisch, C. Rueden, S. Saalfeld, B. Schmid, et al. 2012. Fiji: an open-source platform for biological-image analysis. *Nat. Methods* 9: 676–682.
37. Schröder, K., and T. C. Bosch. 2016. The origin of mucosal immunity: lessons from the holobiont *Hydra. MBio*. DOI: 10.1128/mBio.01184-16.
38. Garcia-Garcia, E., J. Galindo-Villegas, and V. Mulero. 2013. Mucosal immunity in the gut: the non-vertebrate perspective. *Dev. Comp. Immunol.* 40: 278–288.
39. Nyholm, S. V., and J. Graf. 2012. Knowing your friends: invertebrate innate immunity fosters beneficial bacterial symbioses. *Nat. Rev. Microbiol.* 10: 815–827.
40. Tassanakajon, A., K. Somboonwiwat, P. Supungul, and S. Tang. 2013. Discovery of immune molecules and their crucial functions in shrimp immunity. *Fish Shellfish Immunol.* 34: 954–967.
41. Robalino, J., J. S. Almeida, D. McKillen, J. Colglazier, H. F. Trent, III, Y. A. Chen, M. E. T. Peck, C. L. Browdy, R. W. Chapman, G. W. Warr, and P. S. Gross. 2007. Insights into the immune transcriptome of the shrimp *Litopenaeus vannamei*: tissue-specific expression profiles and transcriptomic responses to immune challenge. *Physiol. Genomics* 29: 44–56.
42. Cash, H. L., C. V. Whitham, C. L. Behrendt, and L. V. Hooper. 2006. Symbiotic bacteria direct expression of an intestinal bactericidal lectin. *Science* 313: 1126–1130.
43. Vaishnava, S., M. Yamamoto, K. M. Severson, K. A. Ruhn, X. Yu, O. Koren, R. Ley, E. K. Wakeland, and L. V. Hooper. 2011. The antibacterial lectin RegIIIgamma promotes the spatial segregation of microbiota and host in the intestine. *Science* 334: 255–258.
44. Dinh, C., T. Farinholt, S. Hirose, O. Zhuchenko, and A. Kuspa. 2018. Lectins modulate the microbiota of social amoebae. *Science* 361: 402–406.
45. Pang, X., X. Xiao, Y. Liu, R. Zhang, J. Liu, Q. Liu, P. Wang, and G. Cheng. 2016. Mosquito C-type lectins maintain gut microbiome homeostasis. *Nat. Microbiol.* DOI: 10.1038/nmicrobiol.2016.23.
46. Smith, V. J., and N. A. Ratcliffe. 1980. Cellular defense reactions of the shore crab, *Carcinus maenas*: *in vivo* hemocytic and histopathological responses to injected bacteria. *J. Invertebr. Pathol.* 35: 65–74.
47. van de Braak, C. B. T., M. H. A. Botterblom, N. Taverne, W. B. van Muiswinkel, J. H. W. M. Rombout, and W. P. W. van der Knaap. 2002. The roles of haemocytes and the lymphoid organ in the clearance of injected *Vibrio* bacteria in *Penaeus monodon* shrimp. *Fish Shellfish Immunol.* 13: 293–309.
48. Fujita, T., M. Matsushita, and Y. Endo. 2004. The lectin-complement pathway--its role in innate immunity and evolution. *Immunol. Rev.* 198: 185–202.
49. Johnson, P. T. 1987. A review of fixed phagocytic and pinocytotic cells of decapod crustaceans, with remarks on hemocytes. *Dev. Comp. Immunol.* 11: 679–704.
50. Koiwai, K., H. Kondo, and I. Hirono. 2018. The immune functions of sessile hemocytes in three organs of kuruma shrimp *Marsupenaeus japonicus* differ from those of circulating hemocytes. *Fish Shellfish Immunol.* 78: 109–113.